Downloaded from jnm.snmjournals.org by on March 15, 2017. For personal use only.

Volumetric Analysis of ^{18}F-FDG PET in Glioblastoma Multiforme: Prognostic Information and Possible Role in Definition of Target Volumes in Radiation Dose Escalation

Kevin S. Tralins, MD[1]; James G. Douglas, MD, MS[1]; Keith J. Stelzer, MD, PhD[1]; David A. Mankoff, MD[2]; Daniel L. Silbergeld, MD[3]; Robert Rostomilly, MD[3]; Sharon Hummel, MS[1]; Jeff Scharnhorst, BS[4]; Kenneth A. Krohn, PhD[2]; and Alexander M. Spence, MD[4]

[1]Department of Radiation Oncology, University of Washington Medical Center, Seattle, Washington; [2]Department of Nuclear Medicine, University of Washington Medical Center, Seattle, Washington; [3]Department of Neurosurgery, University of Washington Medical Center, Seattle, Washington; and [4]Department of Neuro-Oncology, University of Washington Medical Center, Seattle, Washington

The use of ^{18}F-FDG PET for brain tumors has been shown to be accurate in identifying areas of active disease. Radiation dose escalation in the treatment of glioblastoma multiforme (GBM) may lead to improved disease control. On the basis of these premises, we initiated a pilot study to investigate the use of ^{18}F-FDG PET for the guidance of radiation dose escalation in the treatment of GBM. **Methods:** Patients were considered eligible to participate in the study if they had a diagnosis of GBM, were at least 18 y old, and had a score of at least 60 on the Karnofsky Scale. Patients were treated with standard conformal fractionated radiotherapy (1.8 Gy per fraction, to 59.4 Gy), with volumes defined by MRI. At a dose of 45–50.4 Gy, patients underwent ^{18}F-FDG PET for boost target delineation. Final noncoplanar fields (3–4) were designed to treat the volume of abnormal ^{18}F-FDG uptake plus a 0.5-cm margin for an additional 20 Gy (2 Gy per fraction), to a total dose of 79.4 Gy. If no abnormal ^{18}F-FDG uptake was observed, treatment was stopped after the conventional course of 59.4 Gy. Age, Karnofsky score, MRI-based volumes, and ^{18}F-FDG PET volume were analyzed as prognostic variables for time to tumor progression (TTP) and overall survival. ^{18}F-FDG PET volumes and MRI-based volumes were compared to assess concordance. **Results:** For the 27 patients who could be evaluated, median actuarial TTP was 43 wk, and median actuarial survival was 70 wk. On univariate analysis, ^{18}F-FDG PET, T1-weighted MRI gadolinium enhancement (excluding nonenhancing resection cavity), and T2-weighted MRI volumes were significantly predictive of TTP. On multivariate analysis, only ^{18}F-FDG PET volume retained significance for predicting TTP. Similar results were obtained on analysis of these variables as prognostic factors for survival. When ^{18}F-FDG PET–based volumes were compared with MRI-based volumes, a difference of at least 25% was detected in all patients, with all but 2 having smaller ^{18}F-FDG PET volumes. Of patients in whom ^{18}F-FDG uptake was initially present but treatment subsequently failed, 83% demonstrated the first tumor progression within the region of abnormal ^{18}F-FDG uptake. **Conclusion:** In comparison with MRI, ^{18}F-FDG PET defined unique volumes for radiation dose escalation in the treatment of GBM. ^{18}F-FDG PET volumes were predictive of survival and time to tumor progression in the treatment of patients with GBM.

Key Words: glioblastoma multiforme; PET; radiation dose escalation

J Nucl Med 2002; 43:1667–1673

Glioblastoma multiforme (GBM) remains one of the most uniformly fatal of all solid tumors. Radiotherapy treatment of GBM has been shown to increase median survival (*1–3*). However, even with treatment, the overall prognosis remains extremely poor. Trials of radiation dose escalation beyond 60 Gy have not proven beneficial in the treatment of GBM (*4–8*). Presumably, any enhancement of tumor control is undermined by increased toxicity to normal brain tissue. Risk of brain injury after radiation is a function of the volume of brain included within radiation fields, and the most likely site of first recurrence is near the original tumor site. Therefore, there is interest in using conformal techniques to escalate radiation dose to a limited volume containing the highest tumor cell burden.

In previous treatment trials, the volume designated for dose escalation has generally been determined by conventional anatomic imaging such as CT or MRI (*9*). A typical volume for dose escalation beyond 60 Gy has been defined as the operative bed plus the area of gadolinium enhancement on a postoperative T1-weighted MR image. However, the optimal volume to receive the boost dose of radiation has not been determined.

Received Oct. 12, 2001; revision accepted Aug. 8, 2002.

For correspondence or reprints contact: James G. Douglas, MD, Department of Radiation Oncology, University of Washington, 1959 N.E. Pacific St., Box 356043, Seattle, WA 98195-6043.

E-mail: drjay@u.washington.edu

Downloaded from jnm.snmjournals.org by on March 15, 2017. For personal use only.

An incremental improvement in survival by radiation dose escalation will require an expansion of the therapeutic window by targeting the volume at greatest risk for first recurrence while minimizing radiation exposure to functional brain tissue. Newer functional imaging modalities such as PET have been postulated to be more accurate in determining target volumes to guide the radiation treatment of malignancies (*10*). ^{18}F-FDG PET of brain tumors has been shown to be accurate in identifying areas of active disease (*11*,*12*). ^{18}F-FDG uptake correlates with tumor grade and aggressiveness (*11*,*12*), and the level of ^{18}F-FDG uptake in primary brain tumors predicts survival (*13–15*). On the basis of these premises, we initiated a prospective phase I/II trial using ^{18}F-FDG PET uptake as a metabolic marker of the most malignant regions of GBM in determining high-dose-radiation boost volumes for conventionally fractionated conformal external-beam radiation. A comparison of boost target volumes between those determined by ^{18}F-FDG PET and those determined by MRI, along with an analysis of the utility of ^{18}F-FDG PET volume in predicting time to tumor progression (TTP) and survival in GBM patients, is emphasized in this initial evaluation. Our hypotheses are that ^{18}F-FDG PET target volumes are different from MRI-based volumes and that ^{18}F-FDG PET volumes identify foci of active residual tumor. Proving these hypotheses would be of significant clinical relevance, as these foci may represent the source of treatment failure.

MATERIALS AND METHODS

Study Design and Treatment

Patients were considered eligible to participate in the study if they had a diagnosis of GBM, were at least 18 y old, and had a score of at least 60 on the Karnofsky Scale. In a thermoplastic head immobilization mask, patients underwent CT for 3-dimensional computerized radiation treatment planning. Patient positioning was the same for CT as for postoperative MRI. For patients on whom postoperative MRI was performed at a University of Washington institution, MR and CT images were fused within the computerized system, called Prism, that the University of Washington has developed for radiation treatment planning. The initial planning target volume was defined as the T2-weighted MRI signal abnormality plus a 2.5- to 3-cm margin. The initial planning target volume was treated to a dose of 50.4 Gy (1.8 Gy per fraction), usually through 3 noncoplanar fields designed by the beams-eye-view tool of Prism. Fields were then reduced to the second planning target volume, designated as the T2-weighted MRI abnormality plus a 1.5-cm margin. An additional 9 Gy (1.8 Gy per fraction) was delivered to this second planning target volume, bringing the total initial dose to the standard 59.4 Gy. At a dose of between 45 and 50.4 Gy, patients underwent ^{18}F-FDG PET. Because the operative bed anatomy may have changed over the course of radiation, an additional MRI study was performed at the time of the ^{18}F-FDG PET scan for correlation with the ^{18}F-FDG PET images.

All ^{18}F-FDG PET studies were performed on an Advance tomograph (General Electric Medical Systems, Waukesha, WI). Images were acquired in 3 dimensions onto 35 × 128 × 128 matrices using 4-mm transverse and 8.5-mm axial filters. The result was images with 4- to 6-mm spatial resolution in both axial and transverse directions (*16*). ^{18}F-FDG was prepared using the method of Hamacher et al. (*17*) and had radiochemical purity in excess of 95% and specific activity greater than 47 GBq/mmol in all cases. The patients fasted for at least 6 h before the PET study. After plasma glucose measurement to rule out hyperglycemia (glucose less than 150 mg/dL), 259–370 MBq of ^{18}F-FDG were infused over 1–2 min. Starting at approximately 45 min after injection, a 15-min 3-dimensional emission acquisition was obtained, followed by a transmission study 25 min after injection (*16*). Images were acquired with the patients in their radiotherapy head immobilization mask to facilitate coregistration of the PET scans with the treatment-planning CT scans. Images were reconstructed using the manufacturer's implementation of the 3-dimensional reprojection algorithm (*18*). Images were reconstructed in a 30-cm transverse plane by a 14.5-cm axial image field of view onto 128 × 128 × 35 matrices using 4-mm transverse and 8.5-mm axial filters. The resulting image spatial resolution was between 5.5 and 6.5 in full width at half maximum in both axial and transverse directions.

Identification of ^{18}F-FDG–avid areas of tumor and delineation of the ^{18}F-FDG PET–positive contours took place in 2 steps. First, the ^{18}F-FDG–avid tumor areas were determined using MRI as an adjunct to ^{18}F-FDG PET interpretation. Second, ^{18}F-FDG PET images were coregistered to the radiotherapy-planning CT scans, and ^{18}F-FDG–avid tumor contours were drawn on the reformatted ^{18}F-FDG scans. Because patients underwent both PET and CT in the radiotherapy immobilization mask, which firmly constrains head positioning, the reformatted ^{18}F-FDG PET scans used for treatment planning differed only in transverse slice width from the original PET images.

MRI performed close to the time of ^{18}F-FDG PET was used to aid in the interpretation of the ^{18}F-FDG PET studies. When MR images were obtained at the University of Washington and were therefore available in electronic form, the MR and ^{18}F-FDG PET images were software coregistered to aid image interpretation. For MR images obtained elsewhere and available as hard-copy films only, the ^{18}F-FDG PET images were resliced to match the MRI presentation. All ^{18}F-FDG PET images were interpreted by a single observer with expertise in PET imaging of brain tumors. The interpreting physician was aware of patients' clinical characteristics but was generally unaware of patients' conditions over the course of radiotherapy. In accord with prior published studies (*13–15*), ^{18}F-FDG PET images were interpreted by comparing uptake in the tumor region with average uptake in normal white matter, defined as the centrum semiovale contralateral to the tumor.

Areas meeting any of 3 criteria were considered to represent metabolically active tumor. The first criterion was the presence of greater uptake of ^{18}F-FDG in tumor than in normal white matter. To facilitate this determination, images were displayed with both standard gray-scale windowing and with the setting of windowing thresholds to normal white matter uptake levels, as defined above.

The second criterion was the presence of abnormal ^{18}F-FDG uptake within the boundaries of the abnormal region on T2-weighted MR images. Elevated ^{18}F-FDG uptake in areas appearing normal on MRI was considered to be functional rather than tumor based. An example is increased uptake in the visual cortex when it appeared normal on MRI.

The third criterion, applied to the special case of tumor sites in gray matter, when both normal brain and metabolically active

Downloaded from jnm.snmjournals.org by on March 15, 2017. For personal use only.

tumor can have uptake greater than that of white matter, was that only regions with uptake greater than that of white matter and also within the boundaries of MRI contrast enhancement were considered positive. Areas of ^{18}F-FDG uptake in gray matter abnormal only on T2-weighted MRI cannot be reliably classified as tumor versus damaged or edematous gray matter and were therefore not included in the ^{18}F-FDG–avid tumor volume. In contrast, areas with increased ^{18}F-FDG uptake with contrast enhancement indicate tumor, as opposed to the alternate possibilities for a contrast-enhancing region: postsurgical changes or necrosis.

Contours were placed for the ^{18}F-FDG PET–positive boost region by coregistering the ^{18}F-FDG PET images to the treatment planning CT scan using the image manipulation software of Prism. Because patients were scanned in the same head immobilization mask for PET as for CT, only translation and not rotation was allowed in the coregistration process. All coregistrations were confirmed visually by a single experienced observer. Estimated coregistration accuracy, by a comparison of common visualized structures (eye musculature, outer cortical boundaries, etc.), was 1–2 pixels (2–4 mm).

^{18}F-FDG PET tumor volume contours were drawn on the CT-coregistered ^{18}F-FDG PET images using the Prism software and with reference to the original ^{18}F-FDG PET images. The sites of ^{18}F-FDG–avid tumor, identified as described above, were delineated by contours with the following considerations. Contours were drawn to closely encircle all sites of ^{18}F-FDG–avid disease. For lesions with a cold center by ^{18}F-FDG PET, contours were drawn to include the outer rim of increased uptake and to exclude areas in the center without increased uptake. Whenever possible, contours were made to be contiguous within a slice. However, for lesions in which separate, noncontiguous sites of ^{18}F-FDG uptake were seen in the tumor bed, noncontiguous contours were drawn, and the ^{18}F-FDG PET tumor volume was taken as the sum of the volumes of the noncontiguous contours. Once contours were drawn on the individual slices, they were checked for slice-to-slice consistency and adjusted as necessary. In addition, the ^{18}F-FDG PET contours were checked for consistency with the T2-weighted MRI contours to make sure the ^{18}F-FDG PET contours were within the T2-weighted MRI contours to meet the criteria for identifying areas of abnormal tumor uptake.

Final noncoplanar fields (3–4) were designed to treat the volume of abnormal ^{18}F-FDG uptake plus a 0.5-cm margin (the third planning target volume). This final boost volume was treated for an additional 20 Gy (2 Gy per fraction), for a total dose of 79.4 Gy in 43 fractions. When critical structures such as the optic chiasm or optic nerve abutted the final boost volume, margins were adjusted to respect tolerance of these critical structures. If no abnormal ^{18}F-FDG uptake was observed, the treatment was stopped after the conventional course of 59.4 Gy. After completing radiation therapy, patients were followed every 3 mo by clinical examination and MRI. If increased gadolinium enhancement was observed, patients were strongly encouraged to undergo a repeated ^{18}F-FDG PET scan to verify disease progression. ^{18}F-FDG PET confirmed progression if the areas of new contrast enhancement on MRI also had ^{18}F-FDG uptake greater than that of white matter and either not seen on the planning study or qualitatively worse than on the planning study.

Analysis of Correlation Between PET and MRI Volumes

^{18}F-FDG PET volumes were analyzed for size and location and were compared with the MRI-based volumes. Volumes were determined by summation of digitized contours from axial images in Prism. Volumes included in the analysis were T2-weighted MRI signal abnormality, T1-weighted MRI gadolinium enhancement, T1-weighted MRI gadolinium enhancement plus operative cavity, and ^{18}F-FDG PET abnormal activity. Differences in volumes were initially assessed by size criteria using a simple ratio between volumes (i.e., PET volume to MRI volume). When absolute volumes were similar (<25% difference), volume locations were assessed and the degree of volume overlap was determined by a concordance index (CI) as $CI = ([P + M]/X) - 1$, in which P is the boost target volume determined by PET, M is the boost target volume determined by MRI, and X is the volume encompassing the combined ^{18}F-FDG PET (P) and MRI (M) abnormalities. Complete concordance, or equivalence between volumes P, M, and X, would yield a CI of 1 (i.e., $P + M/X = 2$). Conversely, complete nonconcordance would yield a CI of 0 (i.e., volume P and volume M would be entirely separate, and thus $P + M/X = 1$). For example, if the MRI volume measured 10 cm^3 and the PET volume also measured 10 cm^3, by absolute volume the targets would be equivalent. However, to assess volume overlap (concordance), the CI would be applied. If the MRI volume and PET volume were indeed identical, the CI would result in a value of 1 $[([10 + 10]/10) - 1 = 1]$. Alternatively, if the volumes were entirely discordant (no overlap), the CI formula would yield a value of zero $[([10 + 10]/20) - 1 = 0]$. For all other scenarios, the CI would yield a value between 0 and 1, with higher values meaning greater concordance. Values of CI less than 0.75 indicate discordance exceeding 25%. A CI of 1 was assigned if both P and M equaled 0.

Analysis of Potential Prognostic Factors

Age, Karnofsky Scale, T2-weighted MRI volume, T1-weighted MRI gadolinium enhancement volume (both with and without inclusion of the resection cavity), and ^{18}F-FDG PET volume were analyzed as prognostic variables for TTP and survival from date of diagnosis using the Cox proportional hazards model for continuous variables. Statistical analyses were performed using the StatView (1986 version; Abacus Concepts, Inc., Berkeley, CA) software package.

RESULTS

Thirty-eight patients were enrolled in this trial from March 1997 through June 2000. Eight patients either were on treatment or had not received their first follow-up examination and imaging at the time of this analysis. Two pa-

TABLE 1
Characteristics of Patients Who Could Be Evaluated for Volume Analysis

Variable	Mean	Range
Age (y)	46	23–72
Karnofsky Scale	91	70–100
MRI T2-weighted volume (cm^3)	96	7–211
MRI T1-weighted gadolinium volume (cm^3)	23	0–103
MRI T1-weighted gadolinium-plus-cavity volume (cm^3)	32	3–103
^{18}F-FDG PET volume (cm^3)	17	0–93

Downloaded from jnm.snmjournals.org by on March 15, 2017. For personal use only.

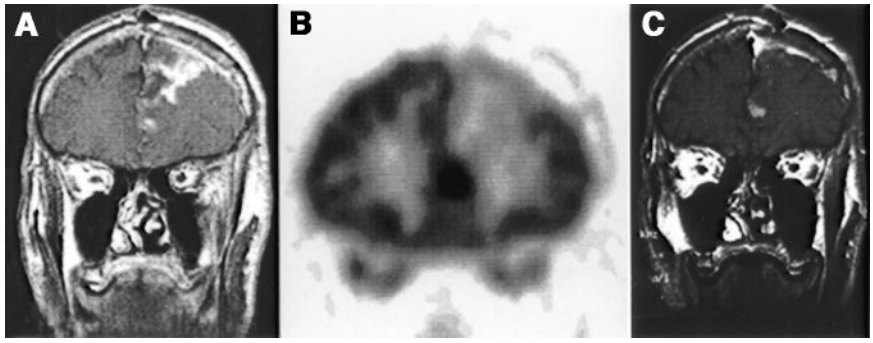


FIGURE 1. (A) Postoperative T1-weighted MR image shows gadolinium-enhanced region. (B) ^{18}F-FDG PET scan after 50.4 Gy of treatment shows activity corresponding to only part of gadolinium-enhanced region. (C) MRI 3 mo after 79.4 Gy of treatment shows diminished gadolinium enhancement in portion of resection cavity that was excluded from boost field on basis of ^{18}F-FDG PET, suggesting that enhancement in this region in A is likely related to postsurgical change as opposed to active tumor.

tients could not undergo MRI: one because of an MRI-incompatible aneurysm clip and the other because of a cardiac pacemaker. The disease of 1 patient progressed before the ^{18}F-FDG PET examination, and the patient was removed from the study. All patients will be included in the final analysis of TTP and survival, but the 27 patients who could be evaluated for MRI and ^{18}F-FDG PET volumes are the focus of this interim analysis. The characteristics of these 27 patients are shown in Table 1.

The comparison of abnormal ^{18}F-FDG PET volume and T1-weighted MRI gadolinium enhancement volume (with and without resection cavity) was of interest to determine whether ^{18}F-FDG PET provided a radiation boost target that was different from that which would have been delineated by MRI. The mean ratio of abnormal ^{18}F-FDG PET uptake to T1-weighted MRI gadolinium enhancement was 0.72, with a range of 0–3.9. The mean ratio of abnormal ^{18}F-FDG PET uptake to T1-weighted MRI gadolinium enhancement plus resection cavity was 0.45, with a range of 0–1.9. The mean abnormal ^{18}F-FDG PET volume was significantly smaller than the T1-weighted MRI gadolinium enhancement volume ($P = 0.0018$) and the T1-weighted MRI gadolinium enhancement plus resection cavity volume ($P = 0.0001$). Often, abnormal ^{18}F-FDG uptake was found within a portion, but not all, of the region of gadolinium enhancement (Fig. 1). Occasionally, ^{18}F-FDG uptake extended outside regions of gadolinium enhancement and partially into regions of T2-weighted MRI signal abnormality (Fig. 2). An example of the PET-delineated volume is shown in Figure 3. The ratio of ^{18}F-FDG PET abnormality volume to T1-weighted MRI gadolinium enhancement volume was outside the range of 0.76–1.24 (i.e., exceeded 25% difference) in all but 4 patients. The CI of the volumes for those 4 patients had a range of 0.47–0.50. The ratio of ^{18}F-FDG PET abnormality volume to T1-weighted MRI gadolinium enhancement plus resection cavity volume was outside the range of 0.76–1.24 for all but 5 patients. The CI of the volumes for those 5 patients had a range of 0.41–0.52. Therefore, the abnormality defined by ^{18}F-FDG PET for escalated radiation dose differed by more than 25% from the volumes that would have been targeted by MRI in all patients who could be evaluated.

Median actuarial TTP for the patients who could be evaluated was 43 wk after diagnosis, and median actuarial survival was 70 wk after diagnosis. Variables of potential prognostic significance for TTP are shown in Table 2. On univariate analysis, ^{18}F-FDG PET, T1-weighted MRI gadolinium enhancement (excluding nonenhancing resection cavity), and T2-weighted MRI volumes were significantly predictive of TTP. Between the 2 potential volumes for guidance of a boost dose of radiation, only the ^{18}F-FDG PET volume retained significance on being entered in a multivariate analysis with T1-weighted MRI gadolinium enhancement volume. Similar results were obtained on analysis of these variables as prognostic factors for survival (Table 3).

Of the 27 patients who could be evaluated, 21 initially demonstrated increased uptake on ^{18}F-FDG PET and 6 did not. Sixteen of the 27 patients who could be evaluated have had tumor progression after radiation. Of patients with tumor progression, 12 initially exhibited abnormal ^{18}F-FDG uptake. Of these 12 patients, the first site of tumor progression was within the region of abnormal ^{18}F-FDG uptake in 10 patients (83%). Of the 6 patients who did not initially

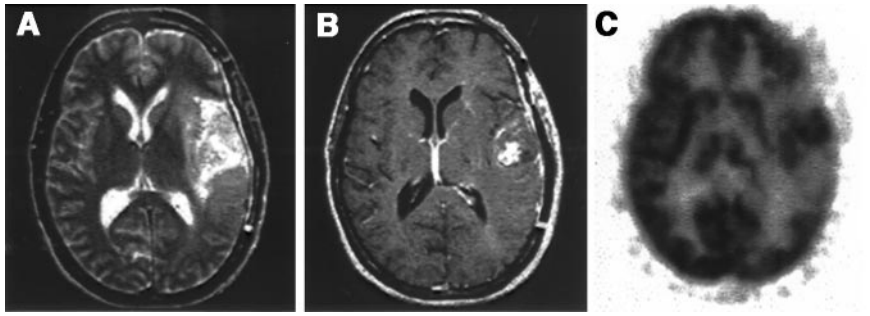


FIGURE 2. (A) T2-weighted MR image obtained at dose of approximately 50 Gy. (B) Corresponding T1-weighted MR image with gadolinium enhancement. (C) PET scan obtained at time of MRI. On PET scan, region of increased uptake extends medially beyond T1-weighted gadolinium enhancement but is contained within region of T2-weighted signal abnormality on MR image.

Downloaded from jnm.snmjournals.org by on March 15, 2017. For personal use only.

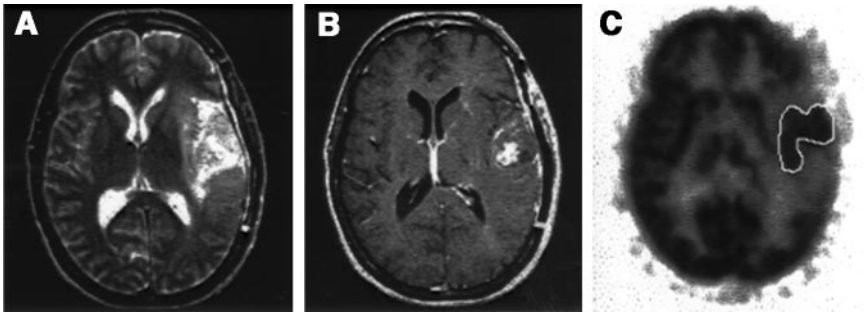


FIGURE 3. (A) T2-weighted MR image obtained at dose of approximately 50 Gy. (B) Corresponding T1-weighted MR image with gadolinium enhancement. (C) PET scan obtained at time of MRI, with PET boost volume outlined.

have an identifiable region of abnormal ^{18}F-FDG uptake on PET, 4 went on to exhibit tumor progression.

DISCUSSION

Local tumor progression in the vicinity of the original site of GBM remains the most prevalent form of failure after treatment. Consequently, there has been great interest in selectively escalating radiation dose to the region of highest risk for subsequent tumor progression. Previous radiation dose escalation trials in the treatment of GBM have used CT and MRI volumes to define targets to receive the highest dose (*9*). These approaches have largely proven unsatisfactory, with no survival benefit demonstrated in multiple trials using a variety of dose-escalation, altered-fractionation, or particle-beam techniques (*4–9,19–24*). The use of biologic imaging, such as PET, magnetic resonance spectroscopy, and SPECT, has been proposed for integration with physical imaging in radiation treatment planning (*25–27*). Our ongoing radiation dose escalation trial has combined biologically guided target definition with computerized 3-dimensional treatment planning for delivery of conformal dose distributions to the volume of interest. This study's hypotheses were that ^{18}F-FDG PET would provide a target for high-dose radiation that differs from that based on anatomic imaging, such as MRI, and that the target defined by ^{18}F-FDG PET would be at significant risk for tumor progression.

The first hypothesis was affirmed by comparing the volumes actually targeted for radiation dose escalation in these patients using ^{18}F-FDG PET with the volumes that would have been defined using gadolinium-enhanced MRI. Volumes defined by ^{18}F-FDG PET were, on average, less than half those defined by the resection cavity plus MRI gadolinium enhancement (the most common technique for defining high-dose radiation volumes in GBM) (*9*). Even if the non–gadolinium-enhancing resection cavity was excluded in defining the MRI volumes, ^{18}F-FDG PET volumes were still an average of 38% smaller. Furthermore, among the minority of patients for whom ^{18}F-FDG PET and MRI volumes were quantitatively similar (less than 25% deviation), the concordance was low. The low CI verified the qualitative observation that ^{18}F-FDG PET regions of interest overlapped some (but not all) regions of gadolinium enhancement on MRI but in some cases also extended outside the gadolinium enhancement into regions of abnormal T2-weighted signal on MRI. Such discordance has recently been described by other investigators and may be of prognostic significance (*28*).

Given the uniqueness of the ^{18}F-FDG PET target volume, a further question is whether this volume actually represents the region most likely to result in improved clinical outcome by an escalating radiation dose in GBM. Ultimately, a randomized clinical trial would be needed to prove a clinical benefit from ^{18}F-FDG PET guidance for radiation dose escalation. However, our preliminary analysis supported the

TABLE 2
Analysis of Potential Prognostic Variables for Tumor Progression After Radiation Therapy for Glioblastoma Multiforme

Variable	Univariate analysis (*P*)	Multivariate analysis (*P*)
Age (y)	0.29	
Karnofsky Scale	0.25	
MRI T2-weighted volume (cm^3)	0.016	
MRI T1-weighted gadolinium volume (cm^3)	0.0033	0.93
MRI T1-weighted gadolinium-plus-cavity volume (cm^3)	0.16	
^{18}F-FDG PET volume (cm^3)	0.0022	0.0022

TABLE 3
Analysis of Potential Prognostic Variables for Survival After Radiation Therapy for Glioblastoma Multiforme

Variable	Univariate analysis (*P*)	Multivariate analysis (*P*)
Age (y)	0.22	
Karnofsky Scale	0.059	
MRI T2-weighted volume (cm^3)	0.037	
MRI T1-weighted gadolinium volume (cm^3)	0.026	0.96
MRI T1-weighted gadolinium-plus-cavity volume (cm^3)	0.094	
^{18}F-FDG PET volume (cm^3)	0.018	0.018

Downloaded from jnm.snmjournals.org by on March 15, 2017. For personal use only.

principle of this technique by demonstrating that ^{18}F-FDG PET volume was more significant than MRI volumes for predicting survival and TTP. This finding confirms those of other investigators. Goldman et al. (*11*) determined that areas of increased ^{18}F-FDG PET activity corresponded well to biopsy-proven anaplastic tumor. Delbeke et al. (*12*) also found that the level of ^{18}F-FDG PET activity corresponded well to pathologic tumor grade. Alavi et al. (*13*) found that ^{18}F-FDG PET was predictive of survival in high-grade glioma, with patients having hypermetabolic lesions on PET imaging surviving a mean of 7 mo, versus 19 mo for patients with hypometabolic lesions. Likewise, in a study of 45 patients with grade III or IV gliomas imaged by ^{18}F-FDG PET (*14*), a mean survival of 5 mo for hypermetabolic lesions was found, versus 19 mo for lesions with lower ^{18}F-FDG uptake. A study performed by Barker et al. (*15*) of patients with recurrent high-grade gliomas showed ^{18}F-FDG PET imaging to be predictive of survival on both univariate and multivariate analysis. In addition to these prior studies showing the level of ^{18}F-FDG uptake in tumor to be predictive of survival, ours is the first study to show that the volume of ^{18}F-FDG–avid tumor is also predictive of outcome. Although the ^{18}F-FDG PET volumes were an indicator of a longer disease-free survival in our study, the rate of false-negative PET studies is worrisome. Four of the 6 patients with a negative PET scan after 45–50 Gy had progressive disease. These 4 represented 25% (4/16) of all patients who progressed, suggesting that PET may identify a smaller cell burden than does MRI but is not an absolute indicator of absent disease.

Because ^{18}F-FDG PET was used for targeting the extra 20 Gy of radiation, it was possible that an enhanced tumor kill could have masked the significance of the ^{18}F-FDG PET volume as a prognostic variable. This potential confounding factor could have been exacerbated by the fact that 6 patients did not have an identifiable region of abnormal ^{18}F-FDG uptake and did not receive the extra radiation dose beyond 59.4 Gy. However, even under these potentially confounding conditions, the volume of abnormal ^{18}F-FDG uptake remained the most significant prognostic variable, strengthening the findings of this preliminary analysis.

Completion of accrual and further follow-up analysis will be needed to determine whether ^{18}F-FDG PET–guided high-dose radiation treatment will be of greater benefit than standard radiotherapy in patients with GBM. The current results support the uniqueness of ^{18}F-FDG PET targeting and confirm the significance of ^{18}F-FDG PET volume as a prognostic variable for patients undergoing treatment for GBM.

CONCLUSION

In comparison with MRI, ^{18}F-FDG PET defined unique volumes for radiation dose escalation in the treatment of GBM. ^{18}F-FDG PET volumes were predictive of survival and TTP in the treatment of patients with GBM.

ACKNOWLEDGMENT

This work was supported by grant P01-CA42045 from the National Institutes of Health.

REFERENCES

1. Walker MD, Alexander E, Hunt WE, et al. Evaluation of BCNU and/or radiotherapy in the treatment of anaplastic gliomas: a cooperative clinical trial. *J Neurosurg.* 1978;49:333–342.
2. Walker MD, Strike TA, Sheline GE. An analysis of dose-effect relationship in the radiotherapy of malignant gliomas. *Int J Radiat Oncol Biol Phys.* 1979;5:1725–1731.
3. Kristiansen K, Hagen S, Kollevold T, et al. Combined modality therapy of operated astrocytomas grade III and IV: confirmation of the value of postoperative irradiation and lack of potentiation of bleomycin on survival time—a prospective multicenter trial of the Scandinavian Glioblastoma Study Group. *Cancer.* 1981;47:649–652.
4. Bleehan NM, Stenning SP. A Medical Research Council trial of two radiotherapy doses in the treatment of grades 3 and 4 astrocytoma. The Medical Research Council Brain Tumour Working Party. *Br J Cancer.* 1991;64:769–774.
5. Nakagawa K, Aoki Y, Fujimaki T, et al. High-dose conformal radiotherapy influenced the pattern of failure but did not improve survival in glioblastoma multiforme. *Int J Radiat Oncol Biol Phys.* 1998;40:1141–1149.
6. Greenberg H, Sandler H, et al. 8000-cGy conformal external beam radiation therapy for malignant astrocytomas [abstract]. *Neurology.* 1995;45(suppl 4): A387.
7. Nelson D, Diener West M, Horton J, et al. Combined modality approach to treatment of malignant gliomas: re-evaluation of RTOG 7401/ECOG1374 with long-term follow-up—a joint study of the RTOG and ECOG. *NCI Monogram.* 1988;6:279–284.
8. Salazar OM, Rubin P, Feldstein ML, Pizzutiello R. High dose radiation in the treatment of malignant gliomas: final report. *Int J Radiat Oncol Biol Phys.* 1979;5:1733–1740.
9. Lee S, Fraass B, Marsh L, et al. Patterns of failure following high dose 3-D conformal radiotherapy for high-grade astrocytomas: a quantitative dosimetric study. *Int J Radiat Oncol Biol Phys.* 1999;43:79–88.
10. Rosenman J. Incorporating functional imaging information into radiation treatment. *Semin Radiat Oncol.* 2001;11:83–92.
11. Goldman S, Levivier M, Pirotte B, et al. Regional glucose metabolism and histopathology of gliomas: a study on positron emission tomography-guided stereotactic biopsy. *Cancer.* 1996;78:1098–1106.
12. Delbeke D, Meyerowitz C, Lapidus R, et al. Optimal cutoff levels of F-18 fluorodeoxyglucose uptake in the differentiation of low-grade from high-grade brain tumors with PET. *Radiology.* 1995;195:47–52.
13. Alavi J, Alavi A, Chawluk J, et al. Positron emission tomography in patients with glioma: a predictor of prognosis. *Cancer.* 1988;62:1074–1078.
14. Patronas NJ, Giovanni DC, Kufta C, et al. Prediction of survival in glioma patients by means of positron emission tomography. *J Neurosurg.* 1985;62:816–822.
15. Barker FG, Chang SM, Valk PE, et al. 18-Fluorodeoxyglucose uptake and survival of patients with suspected recurrent malignant glioma. *Cancer.* 1997; 79:115–126.
16. Lewellen T, Kohlmyer S, Miyaoka R, et al. Investigation of the count rate performance of the General Electric ADVANCE tomograph. *IEEE Trans Nucl Sci.* 1995;42:1051–1057.
17. Hamacher K, Coenen H, Stocklin G. Efficient stereospecific synthesis of no-carrier-added 2-[F-18]-fluoro-2-deoxy-D-glucose using aminopolyether supported nucleophilic substitution. *J Nucl Med.* 1986;27:235–238.
18. Kinahan PE, Rogers JG. Analytic 3D image reconstruction using all detected events. *IEEE Trans Nucl Sci.* 1989;36:964–968.
19. Horiot JC, van den Bogaert W, Ang K, et al. European Organization for Research on Treatment of Cancer trials using radiotherapy with multiple fractions per day: a 1978–1987 survey. *Front Radiat Ther Oncol.* 1988;22:149–161.
20. Ludgate CM, Douglas BG, Dixon PF, et al. Superfractionated radiotherapy in grade III and IV intracranial gliomas. *Int J Radiat Oncol Biol Phys.* 1988;15: 1091–1095.
21. Nieder C, Nestle U, Ketter R, et al. Hyperfractionated and accelerated-hyperfractionated radiotherapy for glioblastoma multiforme. *Radiat Oncol Invest.* 1999;1:36–41.
22. Buatti J, Marcus R, Mendenhall W, et al. Accelerated hyperfractionated radiotherapy for malignant gliomas. *Int J Radiat Oncol Biol Phys.* 1996;34:785–792.

Downloaded from jnm.snmjournals.org by on March 15, 2017. For personal use only.

23. Sneed PK, Gutin PH, Larson DA, et al. Patterns of recurrence of glioblastoma multiforme after external irradiation followed by implant boost. *Int J Radiat Oncol Biol Phys.* 1994;29:719–727.
24. Pickles T, Goodman G, Rheaume D, et al. Pion radiation for high grade astrocytoma: results of a randomized study. *Int J Radiat Oncol Biol Phys.* 1997;37:491–497.
25. Grosu A, Weber W, Feldman H, et al. First experience with I-123-alpha-methyltyrosine SPECT in the 3-D radiation treatment planning of brain gliomas. *Int J Radiat Oncol Biol Phys.* 2000;47:517–526.
26. Ling C, Humm J, Larson S, et al. Towards multidisciplinary radiotherapy (MD-CRT): biological imaging and biological conformity. *Int J Radiat Oncol Biol Phys.* 2000;47:551–560.
27. Gross M, Weber W, Feldmann H, et al. The value of F-18-fluorodeoxyglucose PET for the 3-D radiation treatment planning of malignant gliomas. *Int J Radiat Oncol Biol Phys.* 1998;41:989–995.
28. Vlasenko A, Beattie B, Krol G, Blasberg R. Spatial and volumetric relationship between ^{18}F-FDG hypermetabolism and Gd-DTPA enhancement in patients with recurrent glioma [abstract]. *J Nucl Med.* 2000;41(suppl):217P.

SOCIETY OF NUCLEAR MEDICINE

Downloaded from jnm.snmjournals.org by on March 15, 2017. For personal use only.

JNM The Journal of NUCLEAR MEDICINE

Volumetric Analysis of ^{18}F-FDG PET in Glioblastoma Multiforme: Prognostic Information and Possible Role in Definition of Target Volumes in Radiation Dose Escalation

Kevin S. Tralins, James G. Douglas, Keith J. Stelzer, David A. Mankoff, Daniel L. Silbergeld, Robert Rostomilly, Sharon Hummel, Jeff Scharnhorst, Kenneth A. Krohn and Alexander M. Spence

J Nucl Med. 2002;43:1667-1673.

This article and updated information are available at:
http://jnm.snmjournals.org/content/43/12/1667

Information about reproducing figures, tables, or other portions of this article can be found online at:
http://jnm.snmjournals.org/site/misc/permission.xhtml

Information about subscriptions to JNM can be found at:
http://jnm.snmjournals.org/site/subscriptions/online.xhtml

The Journal of Nuclear Medicine is published monthly.
SNMMI | Society of Nuclear Medicine and Molecular Imaging
1850 Samuel Morse Drive, Reston, VA 20190.
(Print ISSN: 0161-5505, Online ISSN: 2159-662X)

© Copyright 2002 SNMMI; all rights reserved.

SNMMI SOCIETY OF NUCLEAR MEDICINE AND MOLECULAR IMAGING